



HAL
open science

Large mercury release from the Greenland Ice Sheet invalidated

Christian Juncher Jørgensen, Jens Søndergaard, Martin Mørk Larsen, Kristian Kjellerup Kjeldsen, Diogo Rosa, Sarah Elise Sapper, Lars-Eric Heimbürger-Boavida, Stephen Kohler, Feiyue Wang, Zhiyuan Gao, et al.

► **To cite this version:**

Christian Juncher Jørgensen, Jens Søndergaard, Martin Mørk Larsen, Kristian Kjellerup Kjeldsen, Diogo Rosa, et al.. Large mercury release from the Greenland Ice Sheet invalidated. *Science Advances*, 2024, 10 (4), pp.eadi7760. 10.1126/sciadv.adi7760 . hal-04470900

HAL Id: hal-04470900

<https://hal.science/hal-04470900>

Submitted on 21 Feb 2024

HAL is a multi-disciplinary open access archive for the deposit and dissemination of scientific research documents, whether they are published or not. The documents may come from teaching and research institutions in France or abroad, or from public or private research centers.

L'archive ouverte pluridisciplinaire **HAL**, est destinée au dépôt et à la diffusion de documents scientifiques de niveau recherche, publiés ou non, émanant des établissements d'enseignement et de recherche français ou étrangers, des laboratoires publics ou privés.

PHYSICAL SCIENCES

Large mercury release from the Greenland Ice Sheet invalidated

Christian Juncher Jørgensen^{1*†}, Jens Søndergaard¹, Martin Mørk Larsen¹, Kristian Kjellerup Kjeldsen², Diogo Rosa², Sarah Elise Sapper³, Lars-Eric Heimbürger-Boavida⁴, Stephen G. Kohler⁵, Feiyue Wang⁶, Zhiyuan Gao⁶, Debbie Armstrong⁶, Christian Nyrop Albers^{2†}

The major input of mercury (Hg) to the Arctic is normally ascribed to long-range transport of anthropogenic Hg emissions. Recently, alarming concentrations of Hg in meltwater from the Greenland Ice Sheet (GrIS) were reported with bedrock as the proposed source. Reported Hg concentrations were 100 to 1000 times higher than in known freshwater systems of Greenland, calling for independent validation of the extraordinary concentrations and conclusions. Here, we present measurements of Hg at 21 glacial outlets in West Greenland showing that extreme Hg concentrations cannot be reproduced. In contrast, we find that meltwater from below the GrIS is very low in Hg, has minor implications for the global Hg budget, and pose only a very limited risk for local communities and the natural environment of Greenland.

INTRODUCTION

Local glaciers and ice caps in the Northern Hemisphere and the Greenland Ice Sheet (GrIS) have recently been suggested to be important parts of the Arctic mercury (Hg) budget. On the basis of ice-core data, the estimated total Arctic glacial Hg pool is approximately 2400 tonne, approximately 97% of which is in Greenland (1). With Hg concentrations in pre-industrial ice being significantly lower than in ice formed during the 19th and 20th centuries, the dominating source of glacial Hg and input to the Arctic Hg budget is ascribed to long-range transport of anthropogenic Hg emissions (2). In 2021, Hawkings *et al.* (3) claimed to have found a hitherto unaccounted Hg source from the subglacial domain under the GrIS with a calculated annual Hg flux between 3 and 42.5 tonne of dissolved Hg (dHg) from West Greenland alone. Using discharge-weighted mean concentrations of dHg in glacial rivers near Kangerlussuaq and assuming that these are typical of the large Greenland outlet glaciers that dominate discharge of meltwaters from the GrIS, Hawkings *et al.* (3) conclude that “Fluxes of dissolved mercury from the southwestern region of Greenland are estimated to be globally significant, accounting for about 10% of the estimated global riverine flux.”

The elevated Hg concentrations of Hawkings *et al.* (3) (219 to 1750 pM for dHg) stand untested, as very little data exist on Hg concentrations in meltwater rivers draining the GrIS. Compared to Hg concentrations in freshwater rivers of the Arctic, which are known to be several orders of magnitudes lower (2), independent verification of the elevated Hg concentrations in (3) is needed before its fluxes and implications are included in the Arctic or global Hg budget. A fundamental prerequisite for the validity of the upscaling

of “high Hg yields” and the conclusion on global significance of Hawkings *et al.* (3) is that the reported high Hg concentration range, forming the basis for the upscaling model, is reproducible within the included hydrological catchment area during the period of seasonal melt in multiple years.

Here, we expand the sampling of subglacial meltwater from representative outlets at the GrIS to get a better scientific basis for conclusions on the magnitude of glacial Hg sources in Greenland. Samples were collected in 2021 and 2022 over the course of two melt seasons at multiple locations in West Greenland covering both the catchment area of Hawkings *et al.* (3) (“Kangerlussuaq transect” hereafter; see Fig. 1 and fig. S1) and an additional 15 glacial meltwater outlets of variable sizes at the western margin of the GrIS (“West Greenland transect” hereafter), surrounding the study area of Hawkings *et al.* (3) (Fig. 1 and fig. S2). In addition, 12 freshwater samples were collected in South Greenland in 2021 at six auxiliary sampling stations (A1 to A6) within the upscaling area of (3). The samples were analyzed for dHg and total Hg (THg), which represents the sum of dHg and particulate Hg by three independent laboratories in Denmark, France, and Canada (see figs. S3 and S4 and table S3). To investigate the possibility of a large undetected geological Hg source below the GrIS, river sediment was also collected at all meltwater outlets and analyzed for total concentrations of Hg.

RESULTS

Mercury concentrations in glacial meltwater rivers in Western Greenland

Samples of subglacial meltwater from the GrIS were collected to cover (i) the temporal variability of dHg and THg within the Kangerlussuaq transect [sampling station control (Ctrl) 1 to Ctrl 4] and (ii) the spatial variability in Hg concentrations along 15 representative glacial outlets (sampling stations 16 to 74)—the West Greenland transect—at a similar point in time over the melt season (Fig. 1). Linking the two transects to the study sites of Hawkings *et al.* (3), samples were collected twice in 2022 at Isunnguata Sermia [“IS”/station 52, day of year (DOY) 235 and 252] and three times at the Leverett glacier sample station (“LG”/station 53, DOY 128, 232, and 250). All samples were taken in triplicates using precleaned containers and analyzed at

Copyright © 2024 The Authors, some rights reserved; exclusive licensee American Association for the Advancement of Science. No claim to original U.S. Government Works. Distributed under a Creative Commons Attribution NonCommercial License 4.0 (CC BY-NC).

¹Department of Ecoscience, Aarhus University, Roskilde 4000, Denmark. ²Geological Survey of Denmark and Greenland, Copenhagen 1350, Denmark. ³Department of Geosciences and Natural Resource Management, University of Copenhagen; Frederiksberg C, 1958, Denmark. ⁴Aix-Marseille Université, CNRS/INSU, Université de Toulon, IRD, Mediterranean Institute of Oceanography (MIO), Marseille, France. ⁵Department of Chemistry, Norwegian University of Science and Technology (NTNU), Trondheim 7491, Norway. ⁶Centre for Earth Observation Science, and Department of Environment and Geography, University of Manitoba, Winnipeg MB R3T2N2, Canada.

*Corresponding author. Email: cjj@ecos.au.dk
†These authors contributed equally to this work

three independent research laboratories at Aarhus University (AU), CNRS Mediterranean Institute of Oceanography (CNRS-MIO), and University of Manitoba (UM).

Concentrations of THg and dHg were consistently below 15 pM at all sampling events in the Kangerlussuaq transect in the melt seasons of 2021 and 2022, and dHg was frequently below 1 pM. No seasonal trend in THg and dHg was observed in any of the four control stations within the Kangerlussuaq transect in either 2021 or 2022 (see Fig. 2) or at the Isunnguata Sermia and Leverett glaciers (see table S1 showing results from every sampling event from all laboratories). Combined results from the Kangerlussuaq transect show that Hg concentrations are similarly low irrespective of whether the water was sampled (i) at the onset of melting, when the ratio of subglacial meltwater to total discharge is the highest; (ii) before/after peak surface melting of the

GrIS, when dilution by supraglacial water lowers the contribution of subglacial water to total discharge; or (iii) at the end of the melt season, when the relative fraction of subglacial meltwater is increasing once again. The fact that THg and dHg concentrations are consistently low, irrespective of mixing ratios between meltwater sourced from the subglacial and supraglacial domains of varying glacial catchment areas, suggests that the total export of Hg from the subglacial domain feeding the Kangerlussuaq transect is very limited.

At the West Greenland transect, similar low concentrations of THg and dHg were measured (Fig. 3). Concentrations of THg from all laboratories ranged between 3.8 and 27.1 pM, whereas dHg ranged from below the detection limit (<1 pM, AU laboratory) to 2 pM (see tables S1 and S2). At the six additional sampling stations (A1 to A6) in South Greenland (see fig. S3 and S4), concentrations

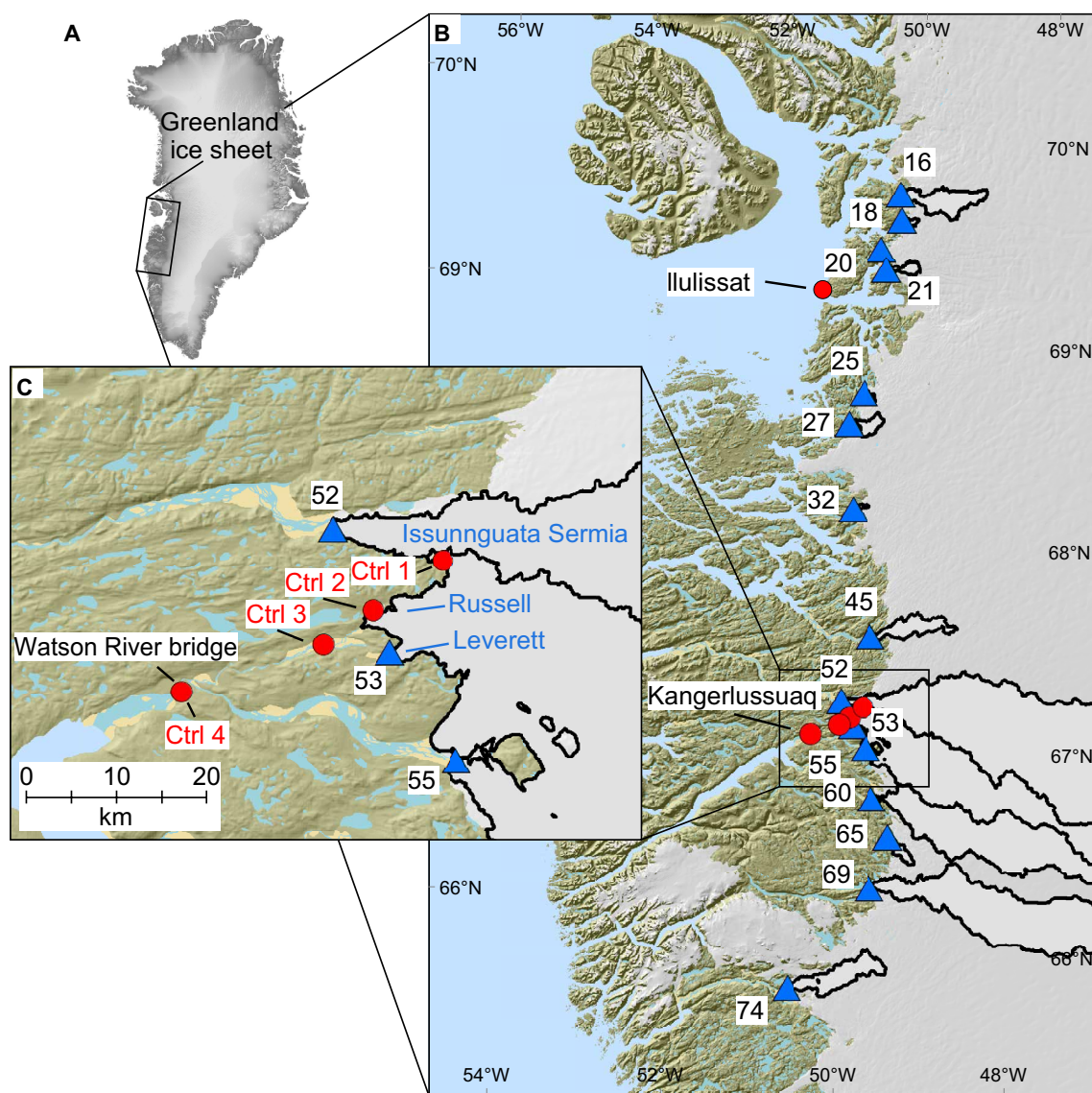


Fig. 1. Map of Greenland showing sampling stations along the western margin of the GrIS. (A) Study region along the GrIS, **(B)** West Greenland transect, and **(C)** Kangerlussuaq transect. Red circles signify the location of sampling stations in the Kangerlussuaq transect. Blue triangles signify the location and number of sampling stations along the West Greenland transect. Black lines signify modeled hydrological catchment area on the GrIS of respective sampling stations.

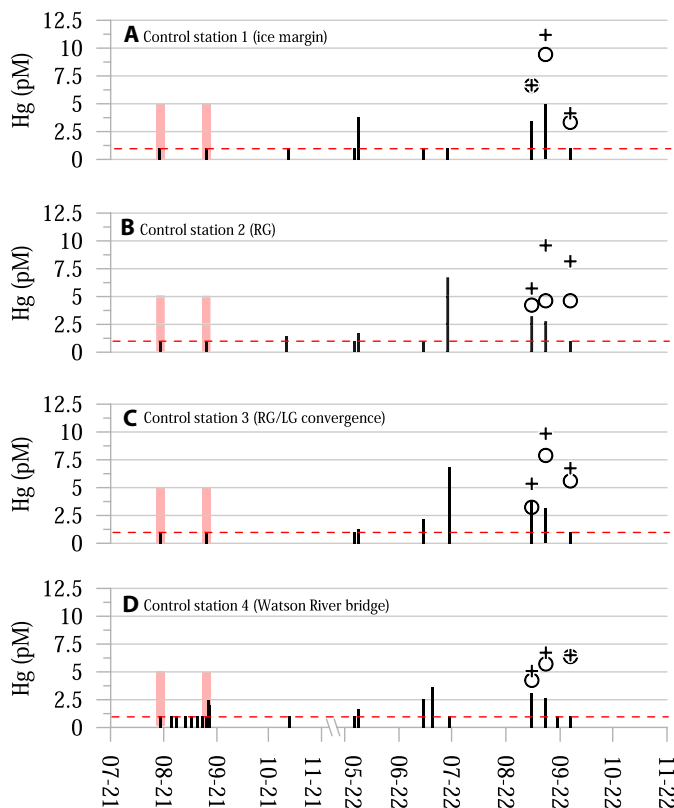


Fig. 2. Temporal variability of THg and dHg at sampling stations in the Kangerlussuaq transect over the melt seasons of 2021 and 2022. (A to D) Samples from control stations 1 to 4, respectively. Note the break on x axis between November 2021 and May 2022. Different symbols indicate different laboratories that conducted the analyses. Black bars: AU (dHg); +: CNRS-MIO (THg); circle: UM (THg). Bars equal to the red dashed line signify “below detection limit (<1 pM, AU laboratory)”. Red bars (2021 only):Eurofins(dHg and THg <5 pM). RG, Russell Glacier; LG, Leverett Glacier.

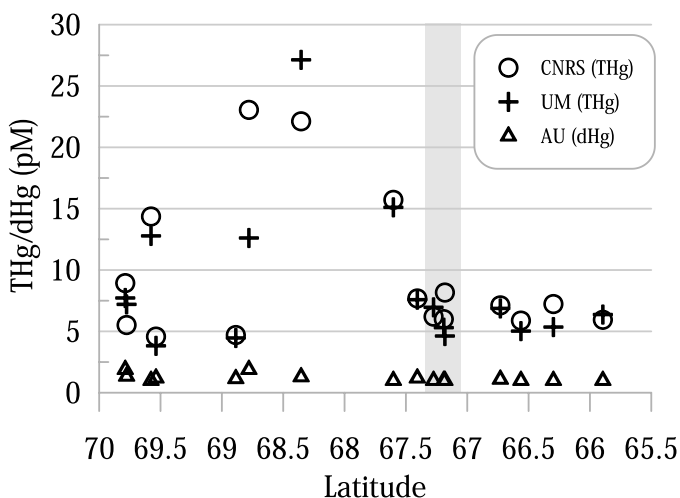


Fig. 3. Spatial variability of THg and dHg along the western margin of the GrIS. The figure shows THg and dHg in 15 glacial meltwater outlets sampled around the Kangerlussuaq transect in August to September 2022 arranged according to latitude. The locations of stations “IS,” “RG,” and “LG” of Hawkins *et al.* (3) are marked in gray shading. IS, Isunnguata Sermia.

of THg and dHg were consistently below the analytical detection limit (<5 pM; Eurofins laboratory).

Hg concentrations in subglacial sediment and marine sedimentary archives, West Greenland

Large geological Hg concentrations are typically found in epithermal and Carlin-type deposits formed at shallow crustal levels (4, 5). These deposits are typically enriched in other chalcophile elements such as arsenic (As), antimony (Sb), and thallium (Tl). In West Greenland, the bedrock is dominated by Archean gneisses, which are expected to extend underneath the ice sheet (6, 7). The geology of West Greenland in general, and of the Kangerlussuaq fjord area specifically, is thus not known or expected to host Hg-bearing minerals, which could release large quantities of Hg.

As a product of basal erosion and mixing of eroded fine particles in the subglacial drainage system, the sediment discharged at the glacier termini will reflect the average geochemistry of the geological source areas below the GrIS. Sediment discharged at the glacier termini may be deposited either in front of glacier termini or in the downstream proglacial river systems (see example in fig. S1) or ultimately discharged to the marine environment. Here, the well-mixed sediment may fall out of suspension and accumulate on the seafloor forming a marine sedimentary archive. Given the typical range of partitioning coefficients between particle-bound and dHg in watersheds, the transport of Hg attached to sediment particles is likely the dominant source of Hg to water bodies that receive Hg from the watershed (8). Should elevated concentrations of Hg be present in the subglacial sediment, it would leave a clear mark in the downstream depositional environments.

On DOY 248 to 251 in 2022, concentrations of THg in subglacial sediment were low [$\leq 1.5 \text{ ng g}^{-1}$ dry weight (dw); see Table 1] at the four control stations and the 15 West Greenland transect sites. Concentrations of As and Sb, chalcophile elements that typically occur jointly with Hg in epithermal and Carlin-type deposits, were below the limit of detection, with the exception of one single sample that yielded an Sb concentration of $16 \mu\text{g g}^{-1}$. The very low Hg, As, and Sb concentrations support the conclusion derived from the analysis of water samples that there is no major subglacial Hg source in the study area.

As opposed to our singular grab samples right at glacier termini, concentrations of Hg in marine sediment represent average conditions over a much larger spatial and temporal catchment area. Should our grab samples for some reason not be able to catch the Hg signal from subglacial erosion of Hg containing bedrock under the GrIS, we would expect it to be detectable in the sedimentary archive close to the GrIS. In 1985 (9), four marine sediment cores were collected in Disko Bay, broadly reflecting in terms of receiving glacial meltwater and suspended sediment in the area where sampling stations st.18, st.20, st.21, st.25, and st.27 are located (see fig. S5). The marine cores were dated using ^{210}Pb and analyzed for Hg (9). While the depth and age profile of the four cores had substantial variation, they also show general similarities. In particular, the core covering the oldest sediment archive (core 7466, 360 years) is located in close proximity to the Kangia Icefjord, which drains the Sermeq Kujalleq ice stream. The Kangia Icefjord is the largest outlet glacier of West Greenland with an estimated drainage basin of $450,000 \text{ km}^2$ accounting for about 20% of the total land area of Greenland (10).

Concentrations of Hg in the marine sediment core 7466, closest to the Sermeq Kujalleq ice stream, were between 50 and 100 ng g^{-1} ,

covering the past 100 years, decreasing to 20 to 40 ng g⁻¹ in the preceding period. A similar observation was made in the “Godthåb fjord” (Nuup Kangerlua), which is south of the location for station 74, although any long-term interpretation is limited by a relatively young sediment core (14 years) due to high sedimentation rates. On the basis of results from 20 cores distributed around Greenland, the study (9) concludes that the Hg concentrations are systematically higher in present-day sediment than in sediment formed 50 to 100 years ago, indicating that anthropogenic emissions and long-range transport of Hg is dominating the input of Hg to the Arctic environment, similar to the conclusion of (1).

The consistent low concentrations of particle-bound Hg in both the recent sediment at the glacier termini and in the marine sedimentary archives suggest an absence of major Hg-bearing minerals in the sediment exported from the subglacial domain of the western margin of the GrIS. Consequently, the combined data does not support the hypothesis of large Hg-rich geological deposits under the western margin of the GrIS.

DISCUSSION

Discrepancy in the range of reported Hg concentrations in glacial meltwater

Combined results from our study show low concentrations of Hg in glacial meltwater from the GrIS, and no evidence of a large and hitherto undetected geogenic source of Hg in neither the glacial sediment from a large number of representative glacial outlets nor the glacial meltwater over space and time nor at depth and time in the marine sedimentary archives.

A large discrepancy thus exists between Hg concentrations measured in this study at a number of representative outlet glaciers at the western margin of the GrIS in 2021 and 2022 (i.e., <1 to 7 pM for dHg) and those reported in Hawkins *et al.* (3) (219 to 1750 pM for dHg). Such a large discrepancy cannot be explained or reconciled by factors such as seasonal/annual variations in meltwater discharge, seasonal variations in subglacial catchment areas, or other hydrological or glaciological features of GrIS.

An alternative explanation for the large discrepancies in meltwater Hg in different studies may be found in methodological considerations as sampling and analysis of Hg in trace concentrations are not trivial and requires special care and attention to avoid sample contamination. In 2021, we sampled water from the Kangerlussuaq transect using Hg-specific sampling protocols, and analyses were done at two independent accredited laboratories in Denmark. In 2022, we took additional meltwater samples close to the outlet portals of the GrIS using a sampling protocol specific for dHg and THg (see Materials and Methods). This protocol includes five field blanks to monitor any potential source of sample contamination during sampling, transport, and analysis, and vials of appropriate material properties were used to minimize any cross-contamination of Hg. In addition, a separate test was performed using both nonacidified and preacidified vials in combination with nonfiltered and in situ field-filtered meltwater. In 2022, identical sets of water samples from both the Kangerlussuaq and West Greenland transects were analyzed at three independent research laboratories in Denmark, France, and Canada. Total Hg concentrations in the travel blanks were all below the analytical detection limit of 1 pM (AU laboratory), confirming no detectable cross contamination during sampling, sample handling, transport,

Table 1. Total concentrations of Hg, As, and Sb in river sediment (s) and dissolved concentrations of As, Sb, and Tl in meltwater (aq). IS, Isunnguata Sermia; RG, Russell Glacier; LG, Leverett Glacier.

| Location | Date | Hg _(s) (ng g ⁻¹) | As _(s) (μg g ⁻¹) | Sb _(s) (μg g ⁻¹) | As _(aq) (μg liter ⁻¹) | Sb _(aq) (μg liter ⁻¹) | Tl _(aq) (μg liter ⁻¹) |
|-------------|----------|--|--|--|---|---|---|
| Ctrl 1 | 9/6/2022 | 0.7 | <12 | <6 | <0.03 | <0.002 | 0.001 |
| Ctrl 2 (RG) | 9/6/2022 | 1.5 | <12 | <6 | <0.03 | <0.002 | 0.001 |
| Ctrl 3 | 9/6/2022 | 0.3 | <12 | <6 | <0.03 | <0.002 | 0.002 |
| Ctrl 4 | 9/6/2022 | 0.5 | <12 | <6 | <0.03 | <0.002 | 0.002 |
| st.16 | 9/5/2022 | 0.2 | <12 | <6 | 0.05 | <0.002 | 0.002 |
| st.18 | 9/5/2022 | 0.3 | <12 | <6 | 0.04 | <0.002 | 0.002 |
| st.20 | 9/5/2022 | 0.2 | <12 | <6 | 0.51 | 0.011 | 0.009 |
| st.21 | 9/5/2022 | 0.2 | <12 | <6 | 0.12 | 0.004 | 0.003 |
| st.25 | 9/5/2022 | 0.4 | <12 | 16 | 0.05 | <0.002 | 0.002 |
| st.27 | 9/5/2022 | 0.3 | <12 | <6 | 0.15 | <0.002 | 0.001 |
| st.32 | 9/8/2022 | 0.8 | <12 | <6 | 0.85 | 0.014 | 0.008 |
| st.45 | 9/8/2022 | 0.3 | <12 | <6 | 0.03 | 0.003 | 0.004 |
| st.52 (IS) | 9/8/2022 | 0.2 | <12 | <6 | 0.07 | 0.004 | 0.013 |
| st.53 (LG) | 9/7/2022 | 0.4 | <12 | <6 | <0.03 | <0.002 | 0.003 |
| st.55 | 9/8/2022 | 0.2 | <12 | <6 | 0.04 | <0.002 | 0.002 |
| st.60 | 9/8/2022 | 1.1 | <12 | <6 | 0.10 | 0.002 | 0.002 |
| st.65 | 9/8/2022 | 0.2 | <12 | <6 | 0.07 | <0.002 | 0.003 |
| st.69 | 9/8/2022 | 1.0 | <12 | <6 | 0.05 | 0.002 | 0.004 |
| st.74 | 9/8/2022 | 0.3 | <12 | <6 | <0.03 | 0.003 | 0.004 |

storage, or sample analysis. Differences in Hg concentrations showed no systematic trend between nonacidified, preacidified, field-filtered, and nonfiltered samples, and concentration levels of Hg were low in all samples (see table S2).

In contrast to our study, the samples of Hawkings *et al.* (3) obtained in 2015 and 2018 used a different and annually varying sampling protocol including field acidification and usage of sampling vials of less suitable material properties (low-density polyethylene bottles, which may be transmissive of various Hg species). In the same field camp and sampling locations as Hawkings *et al.* (3), samples for dissolved methane (CH₄) were obtained in evacuated serum vials, which were prepoisoned with 24 mg of Hg chloride (HgCl₂) (11). It has previously been demonstrated that acidified samples stored in polyethylene bottles may experience markedly increases in THg due to diffusion of elemental Hg through the bottle walls (12, 13).

In Hawkings *et al.* (3), concentration values in field/procedural blanks are only reported for the 2015 campaign. These samples were taken in the field using transported ultra-pure water and the same procedure as the samples. The presence of large Hg concentrations in the field blanks (522 ± 255 pM) indicates that uncontrolled Hg enrichment/contamination of the samples could potentially have taken place during field sampling, field handling, field storage, transport, and/or during analysis. For the 2018 campaign—which provides the most essential data for the general upscaling—only values for the laboratory blanks are reported, whereas essential data on travel/procedural blanks are missing. An important consequence of either missing or very high travel/procedural blanks is the fact that any contamination of the water samples during sampling, field handling/filtration, storage, transport, and/or subsequent analysis cannot be identified and accounted for. Given these uncertainties, it appears plausible that the extremely high Hg concentrations of Hawkings *et al.* (3) could be a product of post-sampling Hg contamination, rather than a representation of in situ concentration levels of Hg in glacial meltwater from the GrIS.

Implications for public health, the environment, and the Arctic Hg budget

Monitoring of Hg in the marine and freshwater ecosystems in Greenland has been performed over several decades in Greenland under the Arctic Monitoring and Assessment Programme, the Greenland Ecosystem Monitoring programme, and various research projects (14–16). Results from these studies show that the natural baseline levels of dHg in riverine systems typically range between 1 and 3 pM, corresponding to the concentration range observed in the glacial meltwater of the current study.

Observations of both THg and dHg in glacier influenced rivers in the Arctic are still limited. However, a current review showed total riverine Hg concentrations (i.e., particulate bound and dHg) in a greater variety of glacier influenced rivers of Alaska and Canada within a typical range of 1 to 100 pM, with only a few being higher (1). At a single location, THg where as high as 2500 pM due to elevated sedimentary Hg levels, while dHg concentrations were within the typical low concentration range (17).

Since the reported concentration range of dHg in meltwater from the GrIS (up to 4000 pM in 2015 and 219 to 1750 pM in 2018) of Hawkings *et al.* (3) cannot be reproduced in neither the Kangerlussuaq transect nor in 15 surrounding glacial meltwater outlets along the western margin of the GrIS or in any other reported glacier influenced rivers of the Arctic, we conclude that the main conclusion

of Hawkings *et al.* (3) is highly inaccurate and that its implications for the magnitude of Hg yield from the GrIS are likely erroneous. Instead, our study documents that glacial meltwater at the western margin of the GrIS contains only very low concentrations of total and dHg, implying that the meltwater poses only a very limited risk for both the local population and natural environment of Greenland.

METHODS AND MATERIALS

Site description

Kangerlussuaq transect

In the melt season of 2021 and 2022, meltwater samples were obtained within the hydrological catchment area of Hawkings *et al.* (3) at four sampling stations representing increasingly larger glacial watersheds (see Fig. 1 and fig. S1). In 2021, samples represent dHg concentrations from DOY 211 (29 July 2021) to 286 (13 October 2021), whereas samples in 2022 represent the period DOY 126 (6 May 2022) to 249 (6 September 2022). The samples collectively represent subglacial meltwater from the initial onset of seasonal melt to the seasonal end of meltwater discharge.

The sampling stations within the Kangerlussuaq transect were distributed with sampling station “control point 1” located at the sample location in (18), which constitutes a lateral glacial outlet of the Isunnguata Sermia glacier. Sampling station “control point 2” is identical to station “RG” in (3), representing glacial runoff from Russell Glacier and the upstream environment. Sampling station “control point 3” is located downstream of the confluence point of the meltwater rivers draining Russell Glacier and Leverett Glacier [station “LG” in (3)]. Sampling station “control point 4” is located at the river bend immediately upstream of the Watson River bridge in Kangerlussuaq, representing the combined meltwater inputs from Russell, Leverett and Isorlersuup glaciers (equal to station 55). Sampling station “control point 4” was sampled with increased sampling frequency over the melt seasons of 2021 and 2022, with a total of 20 sampling events (see Fig. 1 and tables S1 and S2).

By nature of design, the sampling stations control point 1 to control point 4 represent an incrementally increasing catchment area of glacial discharge from the GrIS. By increasing the catchment area and mixing of water from different sources, annual variations in local bed connectivity under the GrIS due to the evolution of the subglacial drainage channel network are expected to average out. Coordinates of sampling stations control point 1 to control point 4 are shown in table S4.

West Greenland transect

Between 5 and 8 September 2022, 15 meltwater rivers of land terminating glaciers of the GrIS surrounding the Kangerlussuaq transect were accessed by helicopter. Coordinates of the sampling locations are listed in table S4. Bordering the Kangerlussuaq transect are the two major outlets of Isunnguata Sermia [named “IS” in Hawkings *et al.* (3)] and Leverett Glacier [named “LG” in Hawkings *et al.* (3)]. In addition to the helicopter-accessed sampling in September 2022, Isunnguata Sermia glacier was sampled with access by foot on DOY 235, while Leverett Glacier was sampled with access by foot on DOY 128, 232, and 250.

South Greenland freshwater samples

In 2021, filtered and nonfiltered water was sampled and analyzed from six additional meltwater rivers in South-West Greenland (see fig. S4 and table S3). Two rivers received meltwater primarily from the GrIS, while meltwater at the four remaining rivers originate from small peripheral glaciers and ice caps. The rivers are located

between the towns of Nuuk and Paamiut and were sampled twice (late June and early September).

Field sampling protocols

Meltwater samples were obtained from the bank of a free-flowing and well-mixed part of the meltwater stream. Fresh gloves were worn during sampling. In 2021, meltwater was sampled simultaneously using two separate sets of sampling equipment and sampling protocols [GEUS/Eurofins (G/E) protocol and AU protocol]. Each set of samples was then analyzed at two separate accredited laboratories in Denmark (Eurofins and AU). In 2022, meltwater was sampled simultaneously using three separate sets of sampling equipment and sampling protocols (AU protocol, CNRS protocol, and UM protocol). Each set of samples was then analyzed at three separate research laboratories (AU, CNRS, and UM). An overview of the laboratory specific analytical detection limits is shown in table S5.

AU (AU protocol) sampling protocol

Discrete meltwater samples were collected in 100- or 250-ml glass bottles with Teflon-lined lids (see also fig. S6). To obtain the water sample, the rinsed bottle was fully submerged until full and capped underwater to avoid any air bubbles in the bottle. Samples were kept cool and dark until analysis in the laboratory.

G/E (G/E protocol) sampling and analytical protocol

Water was sampled in 30-ml acid-washed amber glass vials with gas-tight Teflon-lined screw lids. For each sampling point and time, water was sampled twice: One sample was taken by lowering a vial well below the surface, shaking with the lid on, emptying, and refilling to 90% of the volume of the vial (nonfiltered sample; THg). A second vial was filled by passing water through a 0.45- μm filter (Q-Max polyethersulfone (PES) membrane filter, Frisette, Denmark; dHg) using a syringe that was thoroughly rinsed in the river. The first few milliliters of the filtrate were discarded. Both vials were immediately closed and stored in a cold and dark place until arrival at the commercial laboratory (Eurofins Denmark) within 2 weeks of the sampling date.

CNRS and UM sampling protocol

Discrete meltwater samples were collected into 40-ml glass vials with Teflon-lined lids (see also fig. S6).

Chemical analyses

AU analytical protocol

Water samples were analyzed according to U.S. Environmental Protection Agency (EPA) Method 1631, Revision E (19). A drop of BrCl solution was added to the water sample to oxidize the Hg species to Hg. The surplus of oxidants was removed by two drops of hydroxyl/ ammonium, after which Hg^{2+} was reduced by a SnCl_2 solution and the released Hg(g) was driven by an Argon gas flow to a gold trap, where Hg was amalgamated into the gold. After collection for a pre-set time to preconcentrate Hg from approximately 40 ml of sample, the Hg is thermally desorbed into the atomic fluorescence detector (P.S. Analytical Millennium Merlin, Kent, UK). Detection limits, calculated as three times the SDs on blind samples, are typically 0.1 to 0.2 ng liter^{-1} . The accredited method is validated by participation in the QUASIMEME proficiency testing program, biyearly analyzing three unknown samples in the range 1 to 50 ng liter^{-1} , and using certified reference material (CRM) BCR579 to ensure correct measurements.

CNRS-MIO analytical protocol

Before sampling, the glass vials were muffled at 450°C for 4 hours and the Teflon-lined lids were washed in an acid bath [1% (v/v) double-distilled HCl] to remove Hg traces. Samples received were

stored in the dark at 4°C until analysis. Before THg analysis, samples were inverted to resuspend particles, and 0.5% (v/v) BrCl solution was added to oxidize the samples overnight. After particle settling, the supernatant was directly decanted into a custom-made cold vapor atomic fluorescence spectroscopy (CVAFS) setup (20). The concentration of THg in the water samples was measured according to U.S. EPA Method 1631 at the MIO using a custom-made single gold trap setup described elsewhere (20) within 3 months after sampling. The BrCl reagent was checked for contamination before analysis by using a standard addition protocol. The concentration of THg in all samples was calculated from a six-point calibration curve traceable to National Institute of Standards and Technology (NIST) 3133 standard reference material in previously purged, Hg-free seawater. Standard bracketing of samples with a NIST 3133 matrix spike was used to correct for eventual instrument signal drift and ensure ongoing precision and recovery. Aliquots of CRMs ORMS-5 (Research Council of Canada) and ERM-CA400 (European Reference Materials) were spiked into previously purged Hg-free seawater matrix with recoveries of $94 \pm 8\%$ ($n = 5$) and $112 \pm 8\%$ ($n = 4$), respectively. Field blanks were measured for THg (0.16 ± 0.03 pM, $n = 3$). Samples analyzed in replicate had relative SDs less than 10%. The calculated limit of detection (LOD) was 0.06 pM.

UM analytical protocol

Once received in the laboratory, all samples were stored in the dark at 4°C. Before analysis, sample bottles were agitated to resuspend all particles for homogenization. After the resettlement of the particles, the supernatant of the sample was carefully decanted into new polypropylene tubes (Falcon) and analyzed for THg. Aliquots of the sample were also filtered by 0.22- μm sterile PES filters (Millex) into new polypropylene tubes and analyzed for dHg. The polypropylene tubes used for THg and dHg analysis were randomly tested before use and found very low THg background concentrations (i.e., no instrument response). The analysis of THg and dHg followed the U.S. EPA Method 1631 (19) and was done on a Tekran 2600 Hg analyzer by CVAFS. In general, water samples were treated with BrCl [0.5% (v/v)] oxidation for at least 8 hours before analysis, and the BrCl was made fresh monthly with KBr (A.C.S. Reagent grade, JT Baker) and KBrO_3 (A.C.S. Reagent grade, JT Baker). The excess BrCl was removed by hydroxylamine hydrochloride (ReagentPlus, 99%; Sigma-Aldrich) before the SnCl_2 (Certified ACS, Fisher Chemical) reduction, after which the elemental Hg generated was introduced to CVAFS for quantification. For the purpose of quality assurance, a CRM BCR-579 (Institute for Reference Materials and Measurements, EU) was measured during the analysis and the concentration (1.6 ng liter^{-1}) agreed well with the certified value (1.9 ± 0.5 ng liter^{-1}). The field blanks were measured at 0.19 ± 0.09 pM ($n = 3$) for THg.

Eurofins analytical protocol

Upon arrival at the laboratory, hydrochloric acid was added to the vials. Within another 7 days, the samples were analyzed by cold vapor atomic fluorescence spectrometry (CV-AFS) according to EPA 245.7 CV-AFS method. Data are supplied by the laboratory as signed certificates of analysis under accreditation by the International Laboratory Accreditation Cooperation (ILAC MRA) and DANAK - The Danish Accreditation Fund.

AU in situ filtration and acidification test

For the earliest samples of 2022, a number of water samples were taken in parallel with the raw water sample, which were either filtered and/or acidified in situ in the field to account for potential loss of Hg from nonacidified sampling bottles during transportation back to

Denmark. During this test, a 500 ml of bulk water sample was obtained in a teflon bottle from the bank of a free-flowing and well-mixed part of the meltwater stream, similar to the standard AU protocol. Water was then transferred using a clean plastic syringe to three sample bottles, to which 1 ml of 30% suprapure hydrochloric acid (Merck) had been added in the laboratory to two of the three bottles. For one of the samples, the meltwater was filtered in situ using a Whatman PES 0.45- μm syringe filter using a polypropylene/polyethylene (PP/PE) syringe directly into the preacidified sample bottle. The resulting sample set consisted of the following sample combination: (i) raw water sample that was not filtered or acidified in the field, (ii) raw water (nonfiltered) that was in situ acidified, and (iii) raw water that was filtered and acidified in situ. Once received in the laboratory, the samples were analyzed according to the standard AU analytical protocol. As results show no systematic variation between the treatments and no indication of loss of Hg from the glass bottles during transportation of nonacidified and nonfiltered samples (table S1.2), the field acidification was discontinued in later sampling events, mainly due to the use of helicopters, where acids are usually not permitted on board.

Sediment sampling and analysis

River sediment was collected from the river sides using a plastic spoon and polyethylene sample bags. A total sample volume of 100 to 200 g was collected at each location, and samples were pooled from subsamples taken at three different spots. Samples were subsequently frozen and later freeze-dried and sieved to <2 mm before analyses. Subsamples of approximately 300 mg were analyzed for THg using a Milestone DMA-80 analyzer. All samples were analyzed as duplicates, and the mean value was reported. The CRMs BCR-320R (channel sediment; $850 \pm 90 \text{ ng g}^{-1} \text{ dw}$), BCR-277R (estuarine sediment; $128 \pm 17 \text{ ng g}^{-1} \text{ dw}$), and ERM-CD281 (rye grass; $16.4 \pm 2.2 \text{ ng g}^{-1} \text{ dw}$) were analyzed with the samples for quality assurance/quality control (QA/QC). The measured recovery (mean \pm SD) on the three CRMs were $100 \pm 2\%$ ($n = 5$), $105 \pm 2\%$ ($n = 5$), and $104 \pm 9\%$ ($n = 4$), respectively. The LOD determined as 3 SD on a series of blank samples (empty sample boats) was $0.2 \text{ ng Hg g}^{-1} \text{ dw}$. In addition to the Hg analysis, samples were analyzed for 39 elements using an Olympus Vanta VMR pXRF instrument as described in (21). In this study, only As and Sb are reported. The CRMs NIST 2709a, 2710a, and 2711a were analyzed with the samples for QA/QC. The LODs for As and Sb using this technique are approximately 12 and $6 \mu\text{g g}^{-1} \text{ dw}$, respectively (21). The measured recovery in the three CRMs ($n = 2$ to 3) ranged between 98 and 120% for As and 117 and 120% for Sb.

Freshwater sampling and analysis for other elements than Hg

Immediately after collection, water was filtered through a Whatman PES 0.45- μm syringe filter using a PP/PE syringe and into 15-ml PP vials. Before the sampling, a series of field blanks had been prepared in the laboratory using Milli-Q water filtered through the same filtering system, which were kept with the samples at all times. In the laboratory, samples were acidified to $\text{pH} < 2$ with Merck Suprapure HNO_3 and later analyzed for 61 different elements using an Agilent 7900 ICP-MS. In this study, only As, Sb, and Tl are reported. The CRM SLRS-6 was used for QA/QC, and the LOD was determined as 3 SD on the field blanks. The LODs for As, Sb, and Tl were 0.03, 0.002, and $0.0003 \mu\text{g liter}^{-1}$, respectively. The measured recovery was $87 \pm 3\%$ ($n = 8$) for As. No certified values exist for Sb and Tl in SLRS-6.

Supplementary Materials

This PDF file includes:

Figs. S1 to S6

Tables S1 to S5

REFERENCES AND NOTES

1. A. Dastoor, H. Angot, J. Bieser, J. H. Christensen, T. A. Douglas, L.-E. Heimbürger-Boavida, M. Jiskra, R. P. Mason, D. S. Mc Lagan, D. Obrist, P. M. Outridge, M. V. Petrova, A. Ryjkov, K. A. St. Pierre, A. T. Schartup, A. L. Soerensen, K. Toyota, O. Travnikov, S. J. Wilson, C. Zdanowicz, Arctic mercury cycling. *Nat. Rev. Earth Environ.* **3**, 270–286 (2022).
2. Arctic Monitoring and Assessment Programme (AMAP), *Mercury in the Arctic* (AMAP, 2021), pp. 1–324.
3. J. R. Hawkings, B. S. Linhoff, J. L. Wadham, M. Stibal, C. H. Lamborg, G. T. Carling, G. Lamarche-Gagnon, T. J. Kohler, R. Ward, K. R. Hendry, L. Falteisek, A. M. Kellerman, K. A. Cameron, J. E. Hatton, S. Tingey, A. D. Holt, P. Vinsova, S. Hofer, M. Bulinova, T. Vetrovsky, L. Meire, R. G. M. Spencer, Large subglacial source of mercury from the southwestern margin of the Greenland Ice Sheet. *Nat. Geosci.* **14**, 496–502 (2021).
4. A. H. Hofstra, J. Cline, Characteristics and models for Carlin-type gold deposits. *Rev. Econ. Geol.* **13**, 163–220 (2000).
5. D. A. John, P. G. Vikre, E. A. du Bray, R. J. Blakely, D. L. Fey, B. W. Rockwell, J. L. Mauk, E. D. Anderson, F. T. Graybeal, "Descriptive models for epithermal gold-silver deposits" (U.S. Geological Survey Scientific Investigations Report, 2010).
6. J. N. Coennelly, F. C. Mengel, Evolution of Archean components in the Paleoproterozoic Nagssugtoqidian orogen, West Greenland. *GSA Bulletin* **112**, 747–763 (2000).
7. J. Engström, K. E. S. Klint, Continental collision structures and post-orogenic geological history of the kangerlussuaq area in the southern part of the Nagssugtoqidian orogen, Central West Greenland. *Geosciences* **4**, 316–334 (2014).
8. B. F. Lyon, R. Ambrose, G. Rise, C. J. Maxwell, Calculation of soil-water and benthic sediment partition coefficients for mercury. *Chemosphere* **35**, 791–808 (1997).
9. G. Asmund, S. P. Nielsen, Mercury in dated Greenland marine sediments. *Sci. Total Environ.* **245**, 61–72 (2000).
10. M. A. Cooper, K. Michaelides, M. J. Siebert, J. L. Bamber, Paleofluvial landscape inheritance for Jakobshavn Isbræ catchment, Greenland. *Geophys. Res. Lett.* **43**, 6350–6357 (2016).
11. G. Lamarche-Gagnon, J. L. Wadham, B. S. Lollar, S. Arndt, P. Fietzek, A. D. Beaton, A. J. Tedstone, J. Telling, E. A. Bagshaw, J. R. Hawkings, T. J. Kohler, J. D. Zarsky, M. C. Mowlem, A. M. Anesio, M. Stibal, Greenland melt drives continuous export of methane from the ice-sheet bed. *Nature* **565**, 73–77 (2019).
12. J. L. Parker, N. S. Bloom, Preservation and storage techniques for low-level aqueous mercury speciation. *Sci. Total Environ.* **337**, 253–263 (2005).
13. M. H. Bothner, D. E. Robertson, Mercury contamination of sea water samples stored in polyethylene containers. *Anal. Chem.* **47**, 592–595 (1975).
14. F. Rigét, M. P. Tamstorf, M. M. Larsen, J. Søndergaard, G. Asmund, J. M. Falk, C. Sigsgaard, Mercury (Hg) transport in a high arctic river in Northeast Greenland. *Water Air Soil Pollut.* **222**, 233–242 (2011).
15. J. Søndergaard, M. Tamstorf, B. Elberling, M. M. Larsen, M. R. Mylius, M. Lund, J. Abermann, F. Rigét, Mercury exports from a High-Arctic river basin in Northeast Greenland (74°N) largely controlled by glacial lake outburst floods. *Sci. Total Environ.* **514**, 83–91 (2015).
16. J. Søndergaard, F. Rigét, M. P. Tamstorf, M. M. Larsen, Mercury transport in a low-arctic river in Kobbefjord, West Greenland (64° N). *Water Air Soil Pollut.* **223**, 4333–4342 (2012).
17. S. A. Nagorski, A. W. Vermilyea, C. H. Lamborg, Mercury export from glacierized Alaskan watersheds as influenced by bedrock geology, watershed processes, and atmospheric deposition. *Geochim. Cosmochim. Acta* **304**, 32–49 (2021).
18. J. R. Christiansen, C. J. Jørgensen, First observation of direct methane emission to the atmosphere from the subglacial domain of the Greenland Ice Sheet. *Sci. Rep.* **8**, 16623 (2018).
19. U.S. EPA, Method 1631, Revision E: *Mercury in water by oxidation, purge and trap, and cold vapor atomic fluorescence spectrometry* (U.S. Environmental Protection Agency, EPA-821-R-02-019, 2002), pp. 1–38 (2002).
20. L. E. Heimbürger, J. E. Sonke, D. Cossa, D. Point, C. Lagane, L. Laffont, B. T. Galfond, M. Nicolaus, B. Rabe, M. R. van der Loeff, Shallow methylmercury production in the marginal sea ice zone of the central Arctic Ocean. *Sci. Rep.* **5**, 10318 (2015).
21. J. Søndergaard, C. J. Jørgensen, Field portable X-Ray Fluorescence (pXRF) spectrometry for chemical dust source characterization: Investigations of natural and mining-related dust sources in Greenland (Kangerlussuaq area). *Water Air Soil Pollut.* **232**, 144 (2021).

Acknowledgments: We acknowledge G. Asmund, J. Riis Christiansen, and D. van As for assistance and discussions and Kangerlussuaq International Science Support (KISS) for the help with general logistics. **Funding:** The study was funded by the Danish Environmental

Protection Agency, Arktisk miljøstøtte grant 2021-60763 (to C.J.J.). **Author contributions:** Conceptualization: C.J.J., C.N.A., J.S., M.M.L., K.K.K., F.W., and L.-E.H.-B. Methodology: C.J.J., C.N.A., J.S., M.M.L., K.K.K., L.-E.H.-B., and F.W. Investigation: C.J.J., J.S., C.N.A., S.E.S., F.W., D.A., M.M.L., and L.-E.H.-B. Chemical analysis: M.M.L., D.A., S.G.K., Z.G., J.S., and C.N.A. Visualization: C.J.J., K.K.K., D.R., and F.W. Funding acquisition: C.J.J. and C.N.A. Project administration: C.J.J., C.N.A., and L.-E.H.-B. Writing—original draft: C.J.J., C.N.A., J.S., K.K.K., and D.R. Writing—review and editing: C.J.J., C.N.A., J.S., K.K.K., D.R., S.G.K., F.W., Z.G., and M.M.L. **Competing interests:** The authors declare that they have no competing interests. **Data and materials availability:**

All data needed to evaluate the conclusions in the paper are present in the paper and/or the Supplementary Materials.

Submitted 17 May 2023
Accepted 27 December 2023
Published 26 January 2024
10.1126/sciadv.adi7760